

This document is confidential and is proprietary to the American Chemical Society and its authors. Do not copy or disclose without written permission. If you have received this item in error, notify the sender and delete all copies.

Circular Dichroism Spectroscopic Detection of Ligand Binding Induced Subdomain IB Specific Structural Adjustment of Human Serum Albumin

Journal:	<i>The Journal of Physical Chemistry</i>
Manuscript ID:	jp-2013-067108.R1
Manuscript Type:	Article
Date Submitted by the Author:	n/a
Complete List of Authors:	Zsila, Ferenc; Institute of Molecular Pharmacology, Laboratory of Chemical Pharmacology

SCHOLARONE™
Manuscripts

1
2
3
4
5
6
7
8
9
10
11
12
13
14
15
16
17
18
19
20
21
22
23
24
25
26
27
28
29
30
31
32
33
34
35
36
37
38
39
40
41
42
43
44
45
46
47
48
49
50
51
52
53
54
55
56
57
58
59
60

**Circular Dichroism Spectroscopic Detection of Ligand Binding Induced
Subdomain IB Specific Structural Adjustment of Human Serum Albumin**

Ferenc Zsila

Laboratory of Chemical Pharmacology, Institute of Molecular Pharmacology,
Research Centre for Natural Sciences, POB 17, H-1025, Budapest, Hungary

Corresponding author: Ferenc Zsila
Institute of Molecular Pharmacology, Research Centre for Natural
Sciences,
POB 17, H-1025, Budapest, Hungary
Fax: (+36) 1-438-1145
Email: zsila.ferenc@ttk.mta.hu

Abstract

This work demonstrates for the first time that binding of various compounds within subdomain IB of human serum albumin (HSA) provokes characteristic changes in the near-UV circular dichroism (CD) spectrum of the protein. It can be inferred from the spectroscopic features of difference ellipticity signals and from CD displacement experiments that tyrosine residues located in subdomain IB are the source of the observed CD spectral alterations. It is proposed that inclusion of some ligand molecules (bile acids, dehydroepiandrosterone sulfate, steroidal terpenes, fatty acids, ibuprofen, and gemfibrozil) into the pocket of subdomain IB disrupts the Tyr138-Tyr161 interhelical π - π stacking interaction which is reflected in the CD spectrum. This phenomenon can be utilized for the CD detection of subdomain IB specific binding of endo- as well as exogenous agents and to study the drug binding associated local conformational adaptation of the HSA molecule.

Keywords: human serum albumin; bile acid; carbenoxolone; circular dichroism; dehydroepiandrosterone sulfate; fatty acid; gemfibrozil; glycyrrhetinic acid; ibuprofen; subdomain IB; tyrosine side chain

Abbreviations: CD, circular dichroism; CHN, chenodeoxycholic acid; CRB, carbenoxolone; dehydroepiandrosterone sulfate, (DHEAS); FA, fatty acid; GCHN, glycochenodeoxycholic acid; GLC, 18 β -glycyrrhetinic acid; HSA, human serum albumin; ICD, induced circular dichroism; URS, ursodeoxycholic acid

Introduction

Human serum albumin (HSA) is a ubiquitous constituent of blood serum where it is present in millimolar concentration (~ 0.6 mM). The single polypeptide chain of HSA is folded into a multidomain structure composed from three homologous domains (I-III), each of which is divided into two subdomains, termed A and B, having six and four α -helices, respectively. HSA accounts for the binding and transportation of a large number of chemical entities including pharmaceutical substances as well as endogenous compounds. Two principal drug binding regions of HSA called as Sudlow's sites were described several decades ago and characterized extensively by huge number of solution binding studies.¹⁻⁴ Subsequently, X-ray crystallographic investigations provided high-resolution insight into the architecture and ligand binding properties of these pockets situated in subdomain IIA (site IIA) and IIIA (site IIIA), respectively.⁵⁻¹¹ In addition, the existence of a third, separate ligand binding area, different from the conventional Sudlow's sites has also been suggested by several authors.¹²⁻¹⁷ This binding locus called as the digitoxin site is responsible for the interactions of bile acids, digitoxin, digoxin and related cardenolides.^{16,18,19} Neither the lone tryptophan (Trp214 at site IIA), nor the Tyr411 residue (site IIIA) is associated with the digitoxin site but some other Tyr side chains are strongly involved.¹⁶ Moreover, this area is not identical with the high-affinity fatty acid (FA) binding sites.¹⁸ In line with these features, a recent study using recombinant domains of HSA demonstrated the primary binding of digitoxin to domain I²⁰ which contains five Tyr residues and hosts a low-affinity FA site.^{5,21,22} Very recently, circular dichroism spectroscopic (CD) studies have provided several lines of evidence for the broad ligand recognition ability of the large cleft in subdomain IB (site IB).²³ Beyond a few, crystallographically verified primary ligands of this site including hemin,⁶ a bilirubin photoisomer,⁷ a sulphonamide derivative,⁸ and fusidic acid,⁷ the binding of a diverse

set of additional chemical compounds has been demonstrated such as suramin, dicoumarol, bile acids, biliverdin, camptothecin, teniposide and anthracycline derivatives.²³ A prominent feature of this pocket is its conformational plasticity which allows proper accommodation of structurally divergent compounds.¹³

By employing CD spectroscopy, the present contribution shows that accommodation of certain ligand molecules at site IB induces characteristic changes in the near-UV CD spectrum of the protein which can be well characterised by using the difference CD approach. Subtraction of CD contribution of native HSA from that its ligand-bound form in the near-UV region (250-320 nm) results in a difference ellipticity curve revealing the conformational changes of the aromatic side chains (Trp, Tyr, Phe).²⁴ Such a modification of the CD profile of HSA is related to the unique, residue specific structural adaptation of the binding pocket prompted by inclusion of some guest compounds (Fig. 1). Among that test ligands, bile acids were included due to a previous proposal on their non-conventional albumin binding location¹² as well as their displacing effect observed against HSA-bound biliverdin.²³ Similarly, 18 β -glycyrrhetic acid and carbenoxolone have also showed biliverdin competition indicating their accommodation in the site IB pocket.²³ In addition, peer-reviewed crystallographic data demonstrated the subdomain IB binding of fusidic acid⁷ while inclusion of ibuprofen and gemfibrozil has been postulated based on un-published crystallographic results.¹³

Materials and Methods

Materials

Human serum albumin (Sigma, 97%, A1887, fatty acid-free), 5 β -cholanic acid (Sigma), carbenoxolone disodium salt (Sigma), chenodeoxycholic acid (Sigma), ursodeoxycholic acid (Sigma), sodium glycochenodeoxycholate (Sigma), sodium glycocholate (Sigma), sodium taurocholate (Sigma), dehydroepiandrosterone sulfate (Sigma), diazepam (EGIS Pharmaceuticals Plc.), gemfibrozil (AK-Scientific, Inc.), myristic acid (Sigma), palmitic acid (Sigma), oleic acid (Fluka), fusidic acid sodium salt (Santa Cruz Biotechnology, Inc.), 18 β -glycyrrhetic acid (Sigma), and azapropazone (Curry S, Imperial College, London) were used as supplied. All other chemicals were of analytical grade.

Preparation of ligand and HSA solutions

Stock solutions of water soluble compounds were prepared immediately before use in double distilled water (carbenoxolone, fusidic acid, glycocholate, taurocholate, glycochenodeoxycholate, dehydroepiandrosterone sulfate). DMSO/water mixture (1:1 v/v) were used to dissolve chenodeoxycholic acid, ursodeoxycholic acid, and 18 β -glycyrrhetic acid. The volume of DMSO added into sample solutions never exceeded 5% (v/v) and caused negligible effects on the CD spectra. HSA samples were dissolved in physiological Ringer buffer solution (137 mM NaCl, 2.7 mM KCl, 0.8 mM CaCl₂, 1.1 mM MgCl₂, 1.5 mM KH₂PO₄ and 8.1 mM Na₂HPO₄·12H₂O).

Circular dichroism and UV absorption spectroscopic measurements

CD and absorption spectra were recorded on a Jasco J-715 spectropolarimeter at 25 \pm 0.2 $^{\circ}$ C by the use of a rectangular quartz cell of 1 cm optical pathlength (Hellma, USA). Temperature

control was provided by a Peltier thermostat equipped with magnetic stirring. Each spectrum represents the average of three scans obtained by collecting data at scan speed of 100 nm/min. CD curves of ligand-HSA mixtures were corrected by subtracting spectral contributions of ligand-free HSA ([Fig. 2](#)).

Results

Near-UV CD spectroscopic profile of HSA

Since there are no peptide bond transitions in the near-UV region of proteins (240-320 nm) the CD spectrum gives information about the chiral environment around the aromatic side chains as well as on the asymmetry of disulfide bridges. HSA contains 18 tyrosines, 31 phenylalanines, a lone tryptophan residue (Trp214), and 17 pairs of disulfide bonds. Accordingly, the near-UV CD curve of HSA is the sum of the intrinsic chiroptical contribution of these residues (Fig. 2). In general, Phe side chains display vibrational CD fine structure between 255 and 270 nm (1L_b transition), whereas signals between 275 and 287 nm are attributable to the 1L_b band of the phenolic chromophore of tyrosines. The CD contribution from 285 to 305 nm can be ascribed to the asymmetrically perturbed 1L_a and 1L_b transitions of the indole ring of the Trp residues (disulfide bonds give rise to broad, weak signals throughout the near-UV spectrum). Therefore, the negative peaks resolved around 262 and 268 nm most likely are of Phe origin, while the shoulders near 276 and 283 nm can be assigned to the tyrosyl residues. The low energy, broad negative tail of the CD curve extending to 315 nm represents the disulfide contribution.

Effect of bile acids and steroidal saponins on the near-UV CD spectrum of HSA

Due to the presence of several chiral centers bile acids exhibit intrinsic CD signals which are displayed below 220 nm where the $n-\pi^*$ and $\pi-\pi^*$ transitions of the carboxylate moiety occur. Thus, any ellipticity changes observed in the near-UV CD spectra of bile acid-HSA complexes can exclusively be ascribed to the structural modification of the protein matrix provoked by accommodation of the ligand molecules. In relation to the ligand-free state,

addition of chenodeoxycholic (CHN), ursodeoxycholic (URS) and glycochenodeoxycholic acid (GCHN) substantially changes the CD spectrum of HSA. Upon increasing the bile acid concentration of sample solutions, increase of the ellipticity values of HSA could be observed. The difference ellipticity curves obtained by subtracting the CD contribution of the ligand-free protein from that of the bile acid-HSA complexes display partially resolved negative extrema between 275 and 290 nm together with less intense peaks below 270 nm (Fig. 3). It is to be noted that these spectral changes started to develop upon addition of the first aliquots of bile acid stock solutions.

The less intense difference CD peaks induced by glycocholic and taurocholic acid were displayed only when these ligands were added in excess (Fig. 4).

HSA binding of carbenoxolone (CRB) and 18β -glycyrrhetinic acid (18β -GLC) gave rise to similar results: the difference CD curves exhibited a negative peak and a shoulder around 286 and 282 nm (Fig. 5). Importantly, in protein-free solution no negative signals are shown in the intrinsic CD spectra of these molecules. Distinctly from CRB, the negative ellipticity signals induced by 18β -GLC appeared at higher, around a 1:1 steroid:HSA molar ratio.

Additional steroid ligands of HSA including digoxin and fusidic acid failed to induce any CD spectral changes (data not shown).

HSA binding location of bile acids: evaluation by CD displacement experiments

CD markers of the main drug binding regions of HSA can successfully be employed to identify binding sites of ligand molecules. In protein bound state, these markers display characteristic induced CD (ICD) bands, which decrease upon addition of competing agents indicating a common binding area. The subdomain IB binding of CHN, URS, CRB, and GLC has previously been verified showing competition with the site IB label biliverdin and compound 3.²³ In the literature, however, there are some data on the subdomain IIA and IIIA

binding of bile acids, too.^{25,26} Since these regions also contain tyrosyl residues (Tyr150 in IIA and Tyr411 in IIIA) it may occur that the secondary binding of bile acids to site IIA or IIIA is the source of the observed ellipticity changes. Therefore, azapropazone²⁷ and diazepam,²⁸ the representative marker ligands of site IIA and IIIA were used to address this issue. The site marker-HSA complexes prepared around 0.7:1 drug:HSA ratio exhibit characteristic, polyphasic ICD signals (Fig. 6). Upon addition of bile acids (CHN, URS, glycoCHN, glycocholic acid), the long-wavelength, negative ICD band of azapropazone and diazepam were not affected, but new, negative ellipticity signals induced below 300 nm, superposed on the ICD curves of the HSA bound marker drugs. After correction with the induced ellipticity contribution of the CD labels, the resulting difference bands display very similar shape and position to that found with binary steroid-HSA complexes (Fig. 6).

CD spectroscopic changes induced by HSA association of fatty acids, therapeutic drugs, and dehydroepiandrosterone sulfate

The crystallographically verified seven common binding sites of medium and long-chain nonesterified FAs are asymmetrically distributed across the three domains of HSA (FA sites 1-7).^{5,29} The three highest-affinity sites (2, 4, and 5) are situated at the interface between subdomain IA and IIA, within IIIA, and IIIB, respectively.²¹ The additional, lower-affinity FA sites designated as 1, 3, 6, and 7 are hosted within subdomain IB, IIIA, and IIA/IIIB. According to NMR studies, only the highest-affinity sites are occupied at 2:1 FA:HSA molar ratio but above the ratio of 3:1, population of the lower-affinity sites also begins.²² During titration of HSA samples with concentrated stock solution of myristic, palmitic, and oleic acid, the CD spectrum remained constant up to FA:HSA molar ratio of 3. Above of this value, however, negative difference CD peaks were evolved in parallel with the increase of the FA

concentration in the sample solutions (Fig. 7). No further ellipticity changes were measured after reaching 6 mole equivalents of FA.

The ligand binding pocket of subdomain IIIA preferentially accomodates stick like molecules with a peripheral, negatively charged group³⁰. The antiinflammatory and antilipemic drug ibuprofen and gemfibrozil are considered as stereotypical ligands of this site.^{4,30} Up to 1 mole equivalent of these drugs, no CD spectral changes were detected. Further raising of the drug:HSA ratio resulted in the appearance of multiple, negative difference ellipticity bands below 300 nm (Fig. 8). Since ibuprofen is a chiral molecule, the same titration were performed by using its pure enantiomers, too. (*S*)- and (*R*)-ibuprofen produced very similar CD spectroscopic changes to that obtained with the racemic sample (data not shown). Within the concentration range applied during the titrations, no intrinsic CD signals of the ibuprofen enantiomers could be measured above 250 nm in protein-free buffer solution.

Dehydroepiandrosterone sulfate (DHEAS) is the principal 17-ketosteroid in peripheral blood (~3 μM) where its 95% is bound to HSA (K_a : $6.3 \times 10^4 \text{ M}^{-1}$)³¹. Two sets of HSA binding sites, a primary and a secondary one were found for DHEAS, but their location is still unknown.³¹ Due to the presence of the chirally perturbed saturated ketone moiety, DHEAS exhibits a positive intrinsic CD band of $n-\pi^*$ origin, which completely overlaps with the aromatic CD region of HSA (Fig. 9). Upon addition of DHEAS into albumin solution, this CD peak shows a striking transformation: in relation to the symmetrical, bell shaped curve measured in aqueous buffer, the short-wavelength side of the peak loses intensity and displays a well-resolved vibronic progression (Fig. 9). These prominent spectral alterations can be detected from the beginning of the titration, even at low DHEAS:HSA molar ratios. The ellipticity contribution superposed on the CD band of HSA bound DHEAS can be visualized by a simple arithmetic procedure: subtracting CD values of the steroid recorded in

protein-free state from the spectrum measured with HSA results in a negative difference peak showing very similar shape and position to that obtained with bile acids (*cf.* Fig. 3).

Effect of steroids and gemfibrozil on the near-UV CD profile of hemin-HSA complexes

In analogy with the CD titrations when addition of bile acids generated characteristic ellipticity signals superimposed on the ICD curve of HSA bound site labels (Fig. 6), the effect of bile acids, CRB, GLC, DHEAS and gemfibrozil on the ICD spectrum of hemin-HSA complexes was also studied. The large macrocycle of hemin completely occupies the site IB cavity where it binds with very high affinity ($K_a \sim 10^8 \text{ M}^{-1}$).⁶ Inclusion of hemin induces multiple CD peaks allied to its absorption bands.^{28,32} The broad, negative ICD band of hemin displayed between 250-300 nm showed neither shape nor intensity changes upon addition of these ligands (data not shown). The intrinsic CD peak of DHEAS measured in the presence of hemin-HSA complexes is very similar to that found in Ringer buffer but was red shifted by 5 nm (Fig. 9).

Discussion

Taking into consideration the near-UV CD profile of aromatic protein residues, the spectral perturbations of HSA induced by the association of various steroidal compounds suggests the main contribution of Tyr residues. HSA contains a lone Trp residue in subdomain IIA of which 1L_a and 1L_b electronic transitions overlap extensively with that of tyrosines. However, some spectral features help to distinguish between the Trp and Tyr contributions:³³

- the 1L_a transition of Trp lacks any obvious vibronic structure;
- usually, the 0-0 1L_b band of Trp arise between 288 and 293 nm;
- in contrast to Tyr, the 0-0 1L_b band of Trp is more intense than any of the other 1L_b vibronic bands;
- the vibrational structure between 275-289 nm is characteristic to the 1L_b transitions of Tyr side chains.

Accordingly, the CD spectral perturbation of HSA are associated to the altered stereochemistry of some Tyr residues prompted by the binding of ligand molecules. Distinctly from bile acids which are optically transparent above 220 nm, conjugated ketone chromophores of CRB and GLC show optically active $\pi-\pi^*$ and $n-\pi^*$ transitions between 220 and 370 nm.³⁴ It may occur that conformational adaptation of a chiral ligand at the protein binding site modifies its intrinsic CD pattern. In these molecules, however, the ketone moiety is built in a rigid, steroid framework of which asymmetric centers principally determine their intrinsic CD bands. Thus, the observed CD spectroscopic changes can not be associated to the structural modification of these agents. The similar spectroscopic pattern, two negative CD extrema around 282 and 286 nm, induced by different bile acids and saponines also support this conclusion (Fig. 3-5).

Tyr residues participate in the formation of each principal drug binding region of HSA: Tyr138 and Tyr 161 are involved in the ligand binding of subdomain IB, Tyr150 is located in the binding cavity of subdomain IIA, while Tyr411 interacts with guest molecules accommodated within subdomain IIIA.^{5,9,30,35} Taking into account the CD spectroscopic changes only, it could not be clarified which Tyr residues are responsible for the observed CD spectroscopic changes. In this context, however, CD displacement experiments provide valuable data. In spite of the presence of a site IIA specific marker azapropazone, steroid compounds were able to induce near-UV ellipticity changes (Fig. 6). Similarly, the use of the site IIIA label diazepam was not able to preclude the development of negative CD signals prompted by addition of bile acids. Importantly, long-wavelength ICD band of neither diazepam nor azapropazone vanished indicating the formation of diazepam-bile acid-HSA and azapropazone-bile acid-HSA ternary complexes in which the drug and steroid molecules are bound at distinct sites. These results imply that neither Tyr150 (site IIA) nor Tyr411 (site IIIA) side chain is involved in the observed CD spectroscopic changes.

It is to be noted, however, that hydroxylation pattern of the steroid nucleus in bile acids may affect their binding site preference. Distinctly from CHN and URS, 5 β -cholanic acid lacks any hydroxyl substituent and thus it is the most hydrophobic bile acid. Its addition to diazepam-HSA complexes canceled the induced ellipticity bands of the drug indicating a shared binding area in subdomain IIIA (Suppl. Fig. 1). In accord with this, it has previously been shown that 5 β -cholanic acid enhances the ICD signal of HSA-bound biliverdin due to site IIIA-site IB interdomain cooperative allosteric interaction.²³ Similarly to 5 β -cholanic acid, lithocholic acid which bears only a single hydroxyl group at the 3 α position binds to site IIIA as demonstrated by displacement chromatography and CD competition experiments using the site IIIA label diazepam and various profen drugs.^{26,36} Interestingly, as it is shown in ref. 26 lithocholic acid added even at six-fold

molar excess was not able to completely cancel the negative ICD band of diazepam above 300 nm. At the same time, however, the positive ellipticity peak of the drug below 295 displayed a sign inversion: the final ICD curve recorded at lithocholic acid/diazepam molar ratio of 6 exhibits two, partially resolved negative peaks between 280 and 295 nm which are reminiscent to that measured for bile acid-HSA complexes in the present study.²⁶ This implies that besides subdomain IIIA, an additional lithocholic acid binding site might exist in subdomain IB.

It is also shown that pre-occupation of the cavity of subdomain IB with a hemin molecule cancels the ability of ligand molecules to induce difference CD signals which highlights the role of tyrosyl residues of this binding region. Crystallographic data have showed that accomodation of hemin induces large rotation and un-stacking of the Tyr138 and Tyr161 residues.⁶ In ligand-free state, the subdomain IB cavity is L-shaped due to the interhelical π - π stacking of the phenolic rings, of which ligand binding induced concerted motion transforms the pocket into D-shape allowing enough room to completely engulf the large porphyrin nucleus. Similarly, inclusion of medium and long-chain FAs into the pocket also un-stacks the Tyr residues opening up a hydrophobic tunnel for their alkyl chain^{5,29} (Fig. 10). Due to the strong masking effect of the induced ellipticity band of hemin below 300 nm, the tyrosine related difference ellipticity signals could not be resolved in the CD spectrum. In contrast, these bands can be well observed when the conformational adjustment is induced by optically transparent FA molecules (Fig. 7). The fact that the difference CD bands could only be detected at large excess of FAs (FA/HSA molar ratio > 3) suggest that the highest-affinity FA sites (2 in IA/IIA, 4 in IIIA, and 5 in IIIB) are not involved in this process. The FA binding locus in subdomain IB is among the low-affinity FA sites (1 in IB, 3 in IIIA, 6 in IIA, and 7 in IIA) which are populated above 3:1 FA:HSA ratio.²² It must also be stressed that in contrast to

FA site 1, accommodation of FA molecules at the other low-affinity sites (3, 6, and 7) is associated with more modest conformational changes of the binding residues.²⁹

The CD spectroscopic results refer to that un-stacking of the Tyr residues may also occur upon the site IB binding of bile acids, DHEAS, and steroidal saponines. It seems that proper accommodation of these compounds demands rotation of the Tyr138 and Tyr161 side chains which disrupts the stacking interaction between them. Noticeably, based on unpublished crystallographic data, subdomain IB binding of certain steroid-based therapeutics has been claimed to induce similar conformational re-arrangement of that Tyr residues.¹³

Curiously, HSA binding of ibuprofen above 1:1 molar ratio also induced a characteristic difference CD pattern. According to crystallographic studies, besides the primary binding site in subdomain IIIA, only a single secondary ibuprofen locus was found in the shallow trench at the interface between subdomains IIA and IIB that overlaps the low-affinity FA site 6.³⁰

Solution binding studies employing 2D NMR technique corroborated the association of ibuprofen to these sites but also indicated a third, previously unidentified binding area which corresponds to another low-affinity FA site.²² In addition, as it has been concluded from displacement studies, the specific HSA binding site of glycyrrhizin (the glycosidic form of 18 β -GLC) is largely in common with a low-affinity ibuprofen binding area.³⁷ Taken together, it can be presumed that this site is situated within subdomain IB where the Tyr138 and Tyr161 residues un-stack upon hosting of the ibuprofen ligand explaining the observed CD spectroscopic changes. In concordance with this concept, ibuprofen binding in subdomain IB has also been claimed but neither the experimental method nor the crystal structure of the complex were reported¹³. The same is true for gemfibrozil, the association of which to site IB (and IIIA) has also been described based on unpublished crystallographic data.¹³ It can be assumed that the site IB binding mode of ibuprofen and gemfibrozil is similar to that of FAs:⁵ the apolar portion of the drug molecule is inserted into the hydrophobic sub-chamber created

by un-stacking of the tyrosyl residues, while the carboxylic head forms H-bonds to an adjacent basic side chain, *e.g.* Arg117 (Fig. 10).

It must be emphasized, however, that spatial re-positioning of the Tyr residues is not necessarily occurs during ligand binding to subdomain IB. In contrast to hemin and FAs, X-ray structures of other ligand-HSA adducts showed that site IB accomodation of the steroid antibiotic fusidic acid, 4Z,15E-bilirubin-IX α , and a sulphonamide derivative does not perturb the stacked conformation of the Tyr138-Tyr161 pair.^{7,8} In line with this, the present work demonstrated that HSA association of fusidic acid induces no CD spectroscopic changes. It seems that similarly to fusidic acid, site IB accomodation of the digoxin molecule also requires no conformational adjustment of the tyrosyl residues. Understanding what structural features of ligand molecules promote the sterical re-arrangement of Tyr138 and Tyr161 side chains is still a challenging task for future researches.

Importantly, as the cases of FAs, ibuprofen, gemfibrozil, glyco- and taurocholic acid illustrate, CD spectroscopic changes evolved only in ligand excess may refer to the secondary site IB binding of these agents. In contrast, development of the difference ellipticity peaks below 1:1 ligand:HSA ratio suggests the primary site IB association of guest compounds (*e.g.*, CHN, URS, CRB, DHEAS, see Fig. 3 and 4).

Conclusions

The present study demonstrates the characteristic modification of the near-UV CD spectrum of HSA upon binding of important endogenous as well as therapeutic drug ligands. Taking into consideration these results and previously published data, the observed CD spectroscopic changes are assigned to the Tyr138 and Tyr161 residues of subdomain IB where bile acids, DHEAS, steroidal saponines, FAs, and some pharmaceutical substances are bound. Accommodation of these compounds requires un-stacking of the tyrosine side chains defining a novel binding environment which is accompanied by negative ellipticity signals in the difference CD spectrum. Reported for the first time, this spectroscopic approach can be useful to detect site IB accommodation of HSA ligands (especially steroidal compounds), to study the ligand binding induced local conformational adaptation of the binding pocket, to disclose the formation of ligand_{IB}-ligand_{IIA/IIIA}-HSA ternary complexes, and to differentiate between the primary/secondary subdomain IB binding of guest molecules.

Acknowledgements

The author thank Dr. Orsolya Tőke (Research Centre for Natural Sciences, Budapest, Hungary) and Dr. András Gergely (Semmelweis University, Budapest, Hungary) for gifting bile acid (sodium glycochenodeoxycholate, sodium glycocholate, sodium taurocholate) and dehydroepiandrosterone sulfate samples.

References

- (1) Sudlow, G.; Birkett, D. J.; Wade, D. N. Further Characterization of Specific Drug Binding Sites on Human Serum Albumin. *Mol. Pharmacol.* **1976**, *12*, 1052-1061.
- (2) Sudlow, G.; Birkett, D. J.; Wade, D. N. The Characterization of Two Specific Drug Binding Sites on Human Serum Albumin. *Mol. Pharmacol.* **1975**, *11*, 824-832.
- (3) Fehske, K. J.; Schlafer, U.; Wollert, U.; Muller, W. E. Characterization of an Important Drug Binding Area on Human Serum Albumin Including the High-Affinity Binding Sites of Warfarin and Azapropazone. *Mol. Pharmacol.* **1982**, *21*, 387-393.
- (4) Wanwimolruk, S.; Birkett, D. J.; Brooks, P. M. Structural Requirements for Drug Binding to Site II on Human Serum Albumin. *Mol. Pharmacol.* **1983**, *24*, 458-463.
- (5) Bhattacharya, A. A.; Grune, T.; Curry, S. Crystallographic Analysis Reveals Common Modes of Binding of Medium and Long-Chain Fatty Acids to Human Serum Albumin. *J. Mol. Biol.* **2000**, *303*, 721-732.
- (6) Zunszain, P. A.; Ghuman, J.; Komatsu, T.; Tsuchida, E.; Curry, S. Crystal Structural Analysis of Human Serum Albumin Complexed with Hemin and Fatty Acid. *BMC Struct. Biol.* **2003**, *3*, 6.
- (7) Zunszain, P. A.; Ghuman, J.; McDonagh, A. F.; Curry, S. Crystallographic Analysis of Human Serum Albumin Complexed with 4Z,15E-Bilirubin-IX α . *J. Mol. Biol.* **2008**, *381*, 394-406.
- (8) Buttar, D.; Colclough, N.; Gerhardt, S.; MacFaul, P. A.; Phillips, S. D.; Plowright, A.; Whittamore, P.; Tam, K.; Maskos, K.; Steinbacher, S.; Steuber, H. A Combined Spectroscopic and Crystallographic Approach to Probing Drug-Human Serum Albumin Interactions. *Bioorg. Med. Chem.* **2010**, *18*, 7486-7496.

- (9) Ryan, A. J.; Ghuman, J.; Zunszain, P. A.; Chung, C. W.; Curry, S. Structural Basis of Binding of Fluorescent, Site-Specific Dansylated Amino Acids to Human Serum Albumin. *J. Struct. Biol.* **2011**, *174*, 84-91.
- (10) Curry, S. Lessons from the Crystallographic Analysis of Small Molecule Binding to Human Serum Albumin. *Drug Metab. Pharmacokinet.* **2009**, *24*, 342-357.
- (11) Zhu, L.; Yang, F.; Chen, L.; Meehan, E. J.; Huang, M. A New Drug Binding Subsite on Human Serum Albumin and Drug-Drug Interaction Studied by X-Ray Crystallography. *J. Struct. Biol.* **2008**, *162*, 40-49.
- (12) Takikawa, H.; Sugiyama, Y.; Hanano, M.; Kurita, M.; Yoshida, H.; Sugimoto, T. A Novel Binding Site for Bile Acids on Human Serum Albumin. *Biochim. Biophys. Acta* **1987**, *926*, 145-153.
- (13) Carter, D. C., Crystallographic Survey of Albumin Drug Interaction and Preliminary Applications in Cancer Chemotherapy, in: D.J. Abraham, D.P. Rotella (Eds.), *Burger's Medicinal Chemistry and Drug Discovery*, Seventh Edition, John Wiley & Sons, Inc., 2010, pp. 437-467.
- (14) Sengupta, A.; Hage, D. S. Characterization of Minor Site Probes for Human Serum Albumin by High-Performance Affinity Chromatography. *Anal. Chem.* **1999**, *71*, 3821-3827.
- (15) Sjöholm, I.; Ekman, B.; Kober, A.; Ljungstedt-Pahlman, I.; Seiving, B.; Sjödin, T. Binding of Drugs to Human Serum Albumin: XI. The Specificity of Three Binding Sites as Studied with Albumin Immobilized in Microparticles. *Mol. Pharmacol.* **1979**, *16*, 767-777.
- (16) Fehske, K. J.; Muller, W. E.; Wollert, U. The Location of Drug Binding Sites in Human Serum Albumin. *Biochem. Pharmacol.* **1981**, *30*, 687-692.
- (17) Kragh-Hansen, U. Relations between High-Affinity Binding Sites of Markers for Binding Regions on Human Serum Albumin. *Biochem. J.* **1985**, *225*, 629-638.

- (18) Brock, A. Binding of Digitoxin to Human Serum Albumin: Influence of Free Fatty Acids, Bile Acids, and Protein Unfolding on the Digitoxin-Albumin Interaction. *Acta Pharmacol. Toxicol.* **1976**, *38*, 497-507.
- (19) Datta, P.; Dasgupta, A. Interactions between Drugs and Asian Medicine: Displacement of Digitoxin from Protein Binding Site by Bufalin, the Constituent of Chinese Medicines Chan Su and Lu-Shen-Wan. *Ther. Drug Monit.* **2000**, *22*, 155-159.
- (20) Shi, D.; Jin, Y. X.; Tang, Y. H.; Hu, H. H.; Xu, S. Y.; Yu, L. S.; Jiang, H. D.; Zeng, S. Stereoselective Binding of Mexiletine and Ketoprofen Enantiomers with Human Serum Albumin Domains. *Acta Pharmacol. Sin.* **2012**, *33*, 710-716.
- (21) Simard, J. R.; Zunszain, P. A.; Hamilton, J. A.; Curry, S. Location of High and Low Affinity Fatty Acid Binding Sites on Human Serum Albumin Revealed by NMR Drug-Competition Analysis. *J. Mol. Biol.* **2006**, *361*, 336-351.
- (22) Krenzel, E. S.; Chen, Z.; Hamilton, J. A. Correspondence of Fatty Acid and Drug Binding Sites on Human Serum Albumin: A Two-Dimensional Nuclear Magnetic Resonance Study. *Biochemistry* **2013**, *52*, 1559-1567.
- (23) Zsila, F. Subdomain Ib Is the Third Major Drug Binding Region of Human Serum Albumin: Toward the Three-Sites Model. *Mol. Pharm.* **2013**, *10*, 1668-1682.
- (24) Zsila, F. Aromatic Side-Chain Cluster of Biotin Binding Site of Avidin Allows Circular Dichroism Spectroscopic Investigation of Its Ligand Binding Properties. *J. Mol. Recognit.* **2011**, *24*, 995-1006.
- (25) Farruggia, B.; Garcia, F.; Picó, G. Structural Features of the Hydroxy- and Keto-Disubstituted Bile Salts: Human Serum Albumin Binding. *Biochim. Biophys. Acta* **1995**, *1252*, 59-68.
- (26) Bertucci, C. Enantioselective Inhibition of the Binding of *rac*-Profens to Human Serum Albumin Induced by Lithocholate. *Chirality* **2001**, *13*, 372-378.

- (27) Fehske, K. J.; Jahnchen, E.; Muller, W. E.; Stillbauer, A. Azapropazone Binding to Human Serum Albumin. *Naunyn Schmiedebergs Arch. Pharmacol.* **1980**, *313*, 159-163.
- (28) Dockal, M.; Carter, D. C.; Ruker, F. The Three Recombinant Domains of Human Serum Albumin. Structural Characterization and Ligand Binding Properties. *J. Biol. Chem.* **1999**, *274*, 29303-29310.
- (29) Curry, S. Plasma Albumin as a Fatty Acid Carrier. *Adv. Mol. Cell Biol.* **2004**, *33*, 29-46.
- (30) Ghuman, J.; Zunszain, P. A.; Petitpas, I.; Bhattacharya, A. A.; Otagiri, M.; Curry, S. Structural Basis of the Drug-Binding Specificity of Human Serum Albumin. *J. Mol. Biol.* **2005**, *353*, 38-52.
- (31) Plager, J. E. The Binding of Androsterone Sulfate, Ethiocholanolone Sulfate, and Dehydroisoandrosterone Sulfate by Human Plasma Protein. *J. Clin. Invest.* **1965**, *44*, 1234-1239.
- (32) Beaven, G. H.; Chen, S. H.; d' Albis, A.; Gratzer, W. B. A Spectroscopic Study of the Haemin-Human-Serum-Albumin System. *Eur. J. Biochem.* **1974**, *41*, 539-546.
- (33) Strickland, E. H. Aromatic Contributions to Circular Dichroism Spectra of Proteins. *CRC Crit. Rev. Biochem.* **1974**, *2*, 113-175.
- (34) Koide, M.; Ishii, R.; Ukawa, J.; Tagaki, W.; Tamagaki, S. Structural Features of Inclusion Complexes between Glycyrrhizates and Cyclodextrins. *J. Chem. Soc. Japan* **1997**, 489-496.
- (35) Ryan, A. J.; Chung, C. W.; Curry, S. Crystallographic Analysis Reveals the Structural Basis of the High-Affinity Binding of Iophenoxic Acid to Human Serum Albumin. *BMC Struct. Biol.* **2011**, *11*, 18.

- (36) Bertucci, C.; Andrisano, V.; Gotti, R.; Cavrini, V. Modulation of Chromatographic Performances of HSA-Based Hplc Column by Reversible Binding of Lithocholic Acid. *Chromatographia* **2001**, *53*, 515-518.
- (37) Ishida, S.; Kinoshita, M.; Sakiya, Y.; Taira, Z.; Ichikawa, T. Glycyrrhizin Binding Site on Human Serum Albumin. *Chem. Pharm. Bull. (Tokyo)* **1992**, *40*, 275-278.

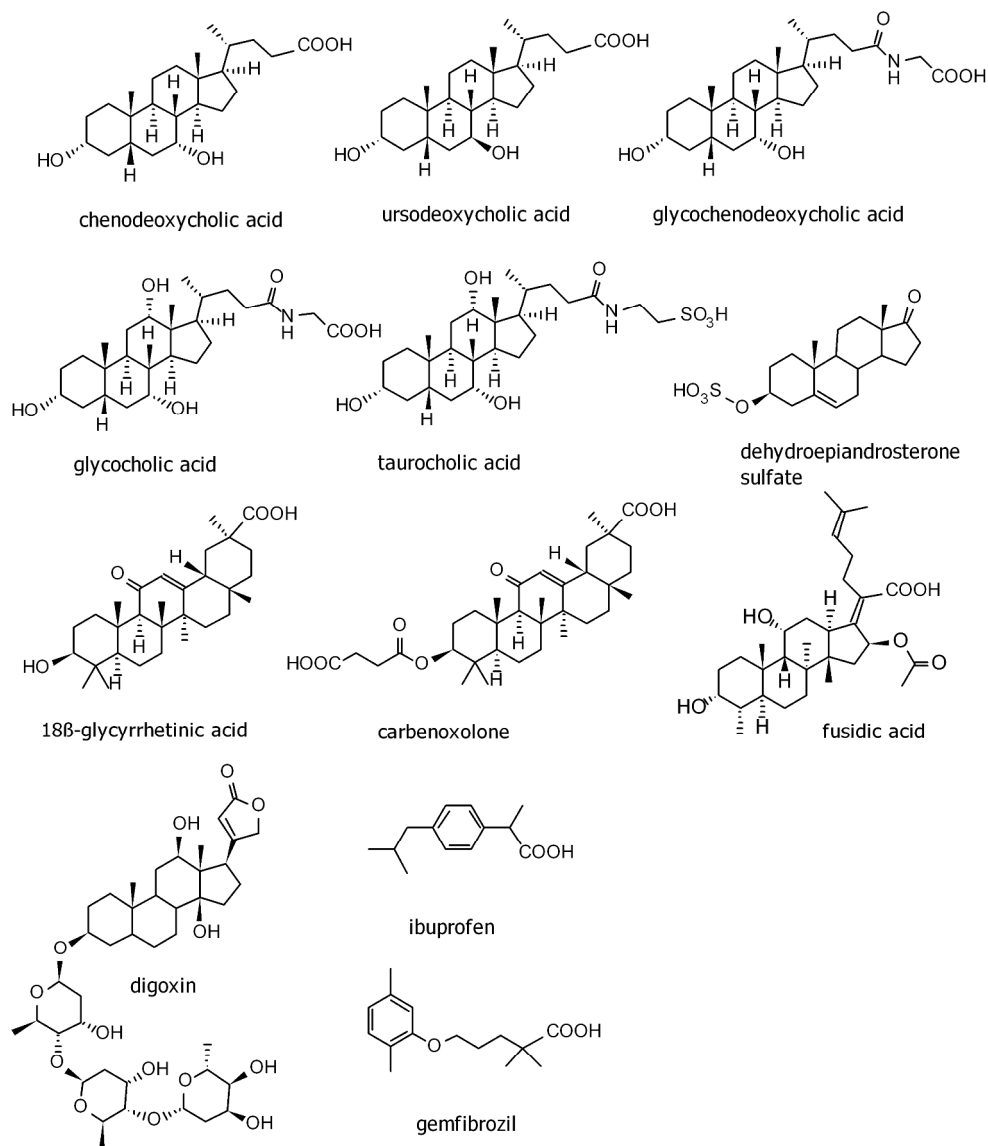


Figure 1
Chemical structures of HSA ligands used in this work.
1211x1420mm (72 x 72 DPI)

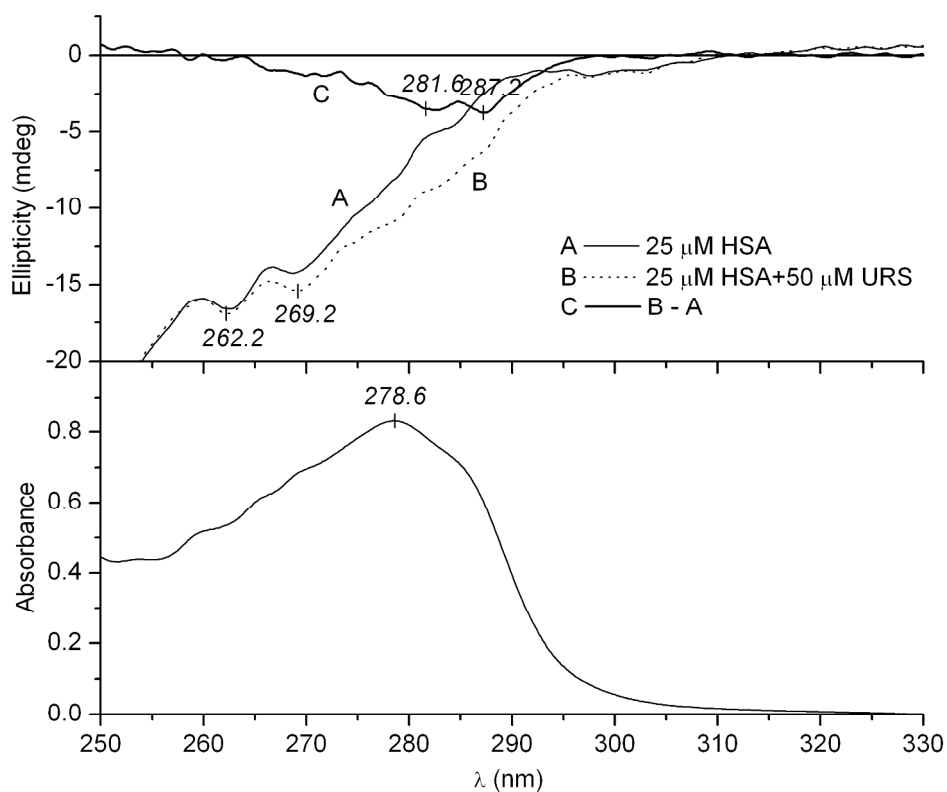


Figure 2
CD and absorption spectra of HSA in the near-UV region measured in the absence and in the presence of ursodeoxycholic acid (Ringer buffer, 25 °C). The difference ellipticity curve ('C') obtained by subtracting CD spectral contributions of the ligand-free HSA ('A') is shown.
232x192mm (300 x 300 DPI)

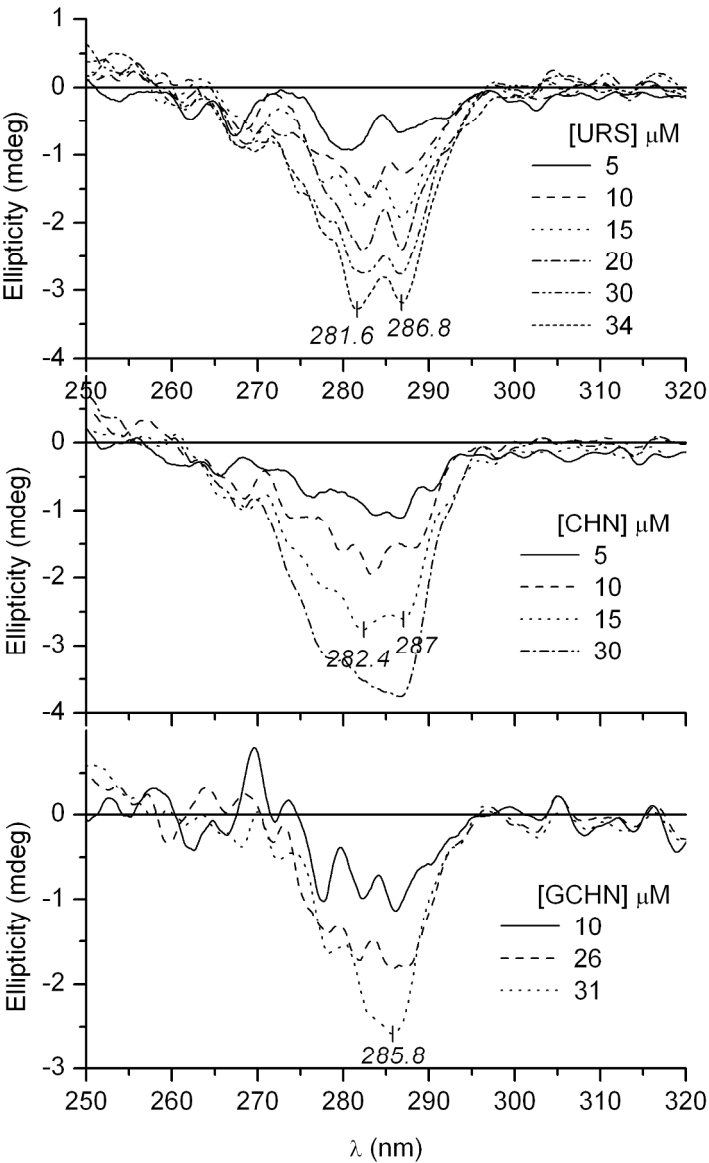


Figure 3
Difference CD curves measured upon stepwise addition of bile acids to 25 μM HSA (Ringer buffer, 25 °C).
163x256mm (300 x 300 DPI)

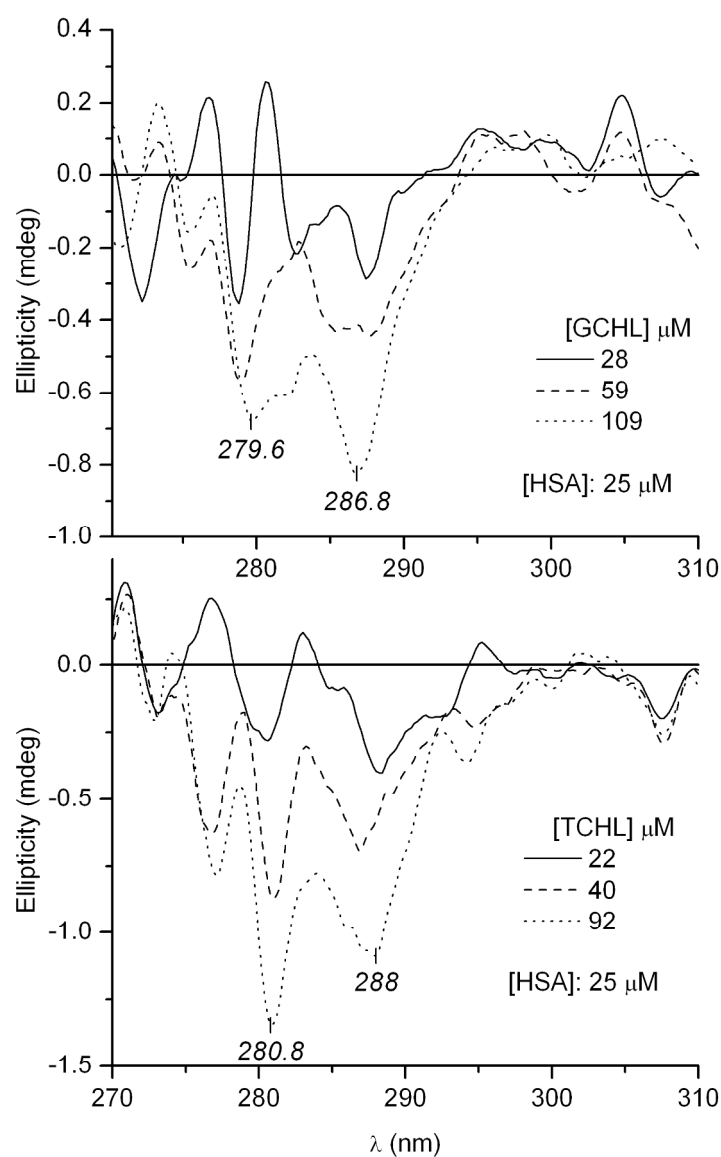


Figure 4
Difference CD curves measured upon stepwise addition of glycocholic (GCHL) and taurocholic acid (TCHL) into HSA solution (Ringer buffer, 25 °C).
167x260mm (300 x 300 DPI)

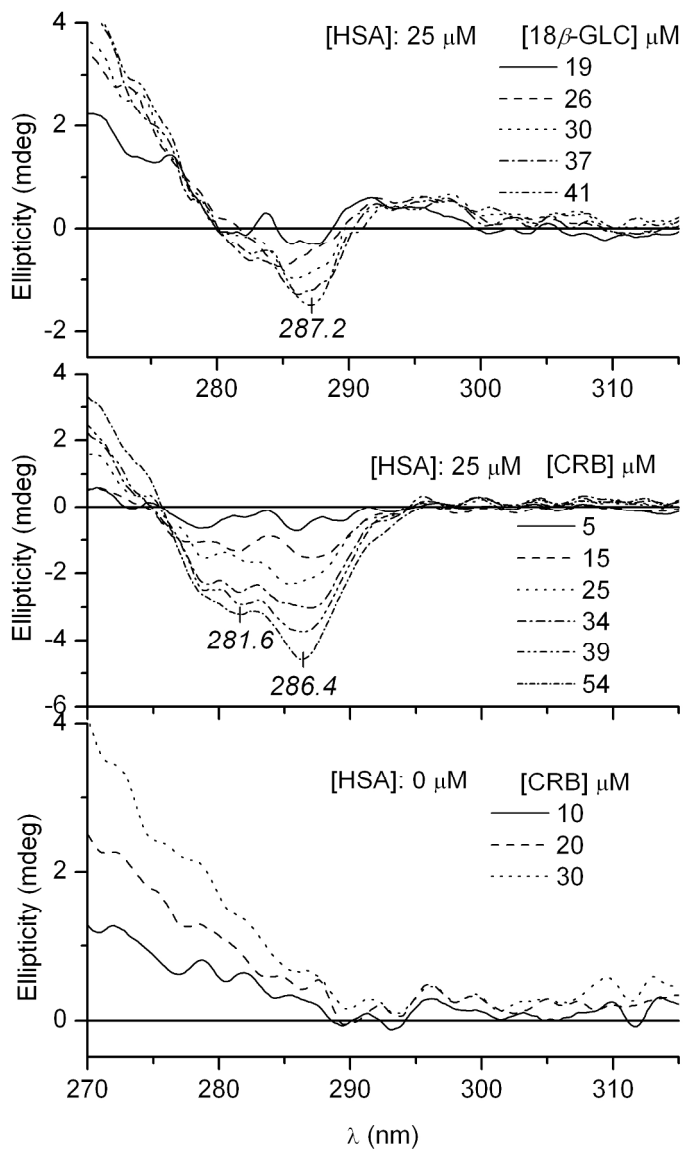


Figure 5
Difference CD curves measured upon stepwise addition of 18β-glycyrrhetic acid (18β-GLC) and carbenoxolone (CRB) to HSA in Ringer buffer at 25 °C. Bottom panel: CD spectra of carbenoxolone in protein-free buffer solution.
159x260mm (300 x 300 DPI)

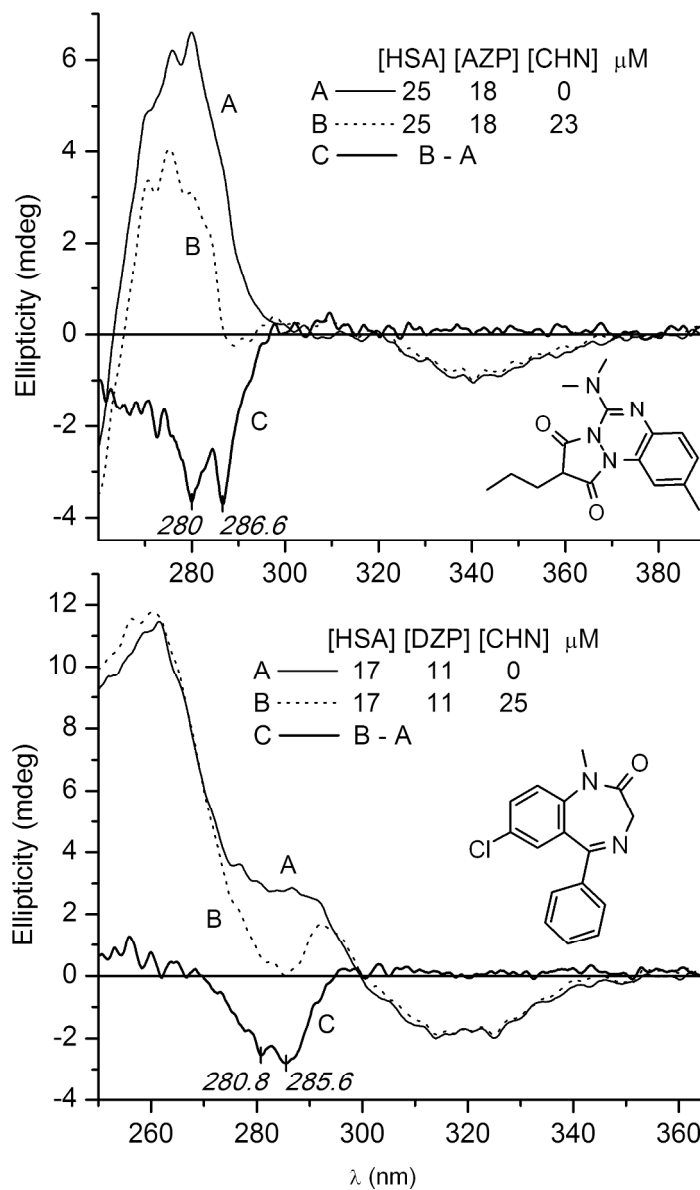


Figure 6

Induced CD curves of azapropazone-HSA (top) and diazepam-HSA (bottom) complexes in the absence ('A') and in the presence ('B') of chenodeoxycholic acid (Ringer buffer, 25 °C). The use of additional bile acids including URS, glycoCHN, and glycocholic acid gave rise to similar results.

352x562mm (150 x 150 DPI)

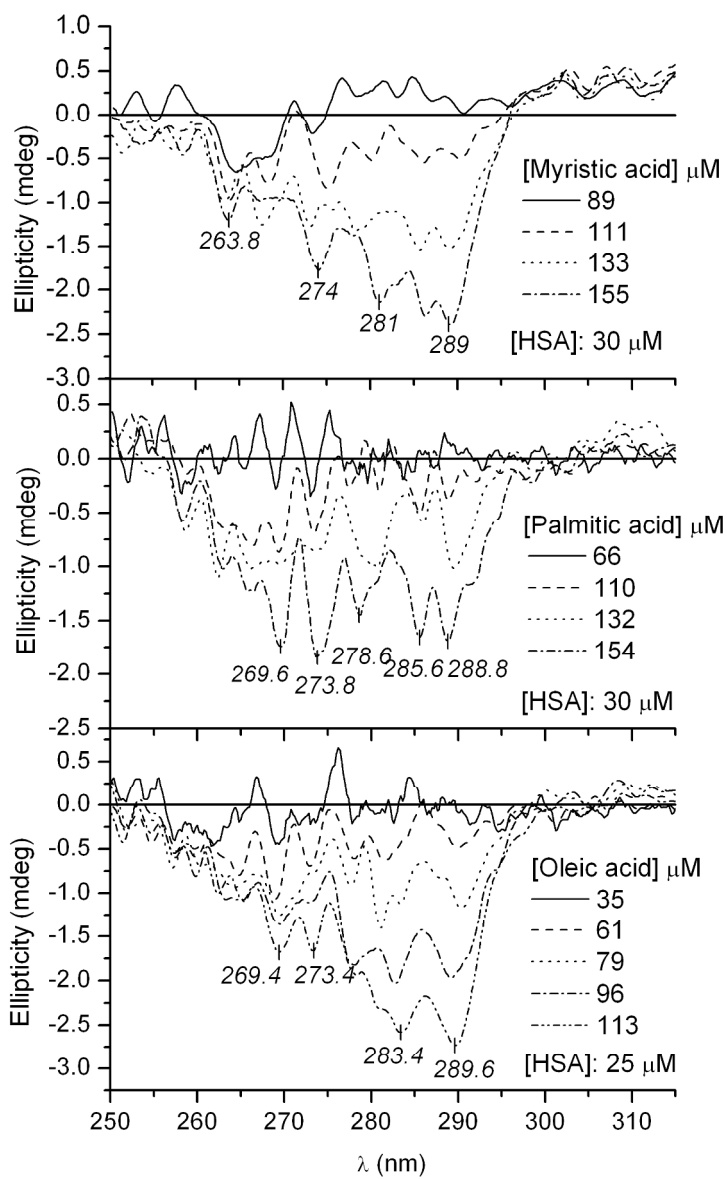


Figure 7
Difference CD spectra measured upon stepwise addition of nonesterified dietary fatty acids into HSA solution
(Ringer buffer, 25 °C).
171x263mm (300 x 300 DPI)

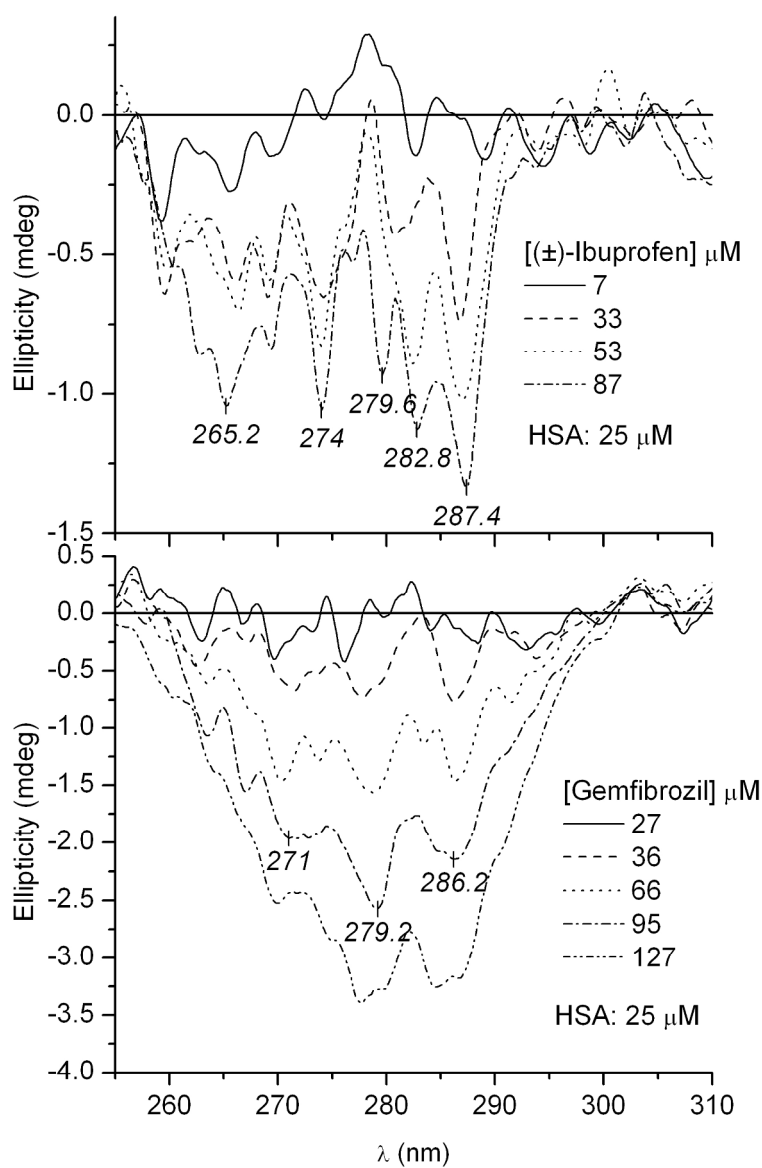


Figure 8
Difference CD spectra measured upon stepwise addition of (±)-ibuprofen and gemfibrozil into HSA solution
(Ringer buffer, 25 $^{\circ}\text{C}$).
175x259mm (300 x 300 DPI)

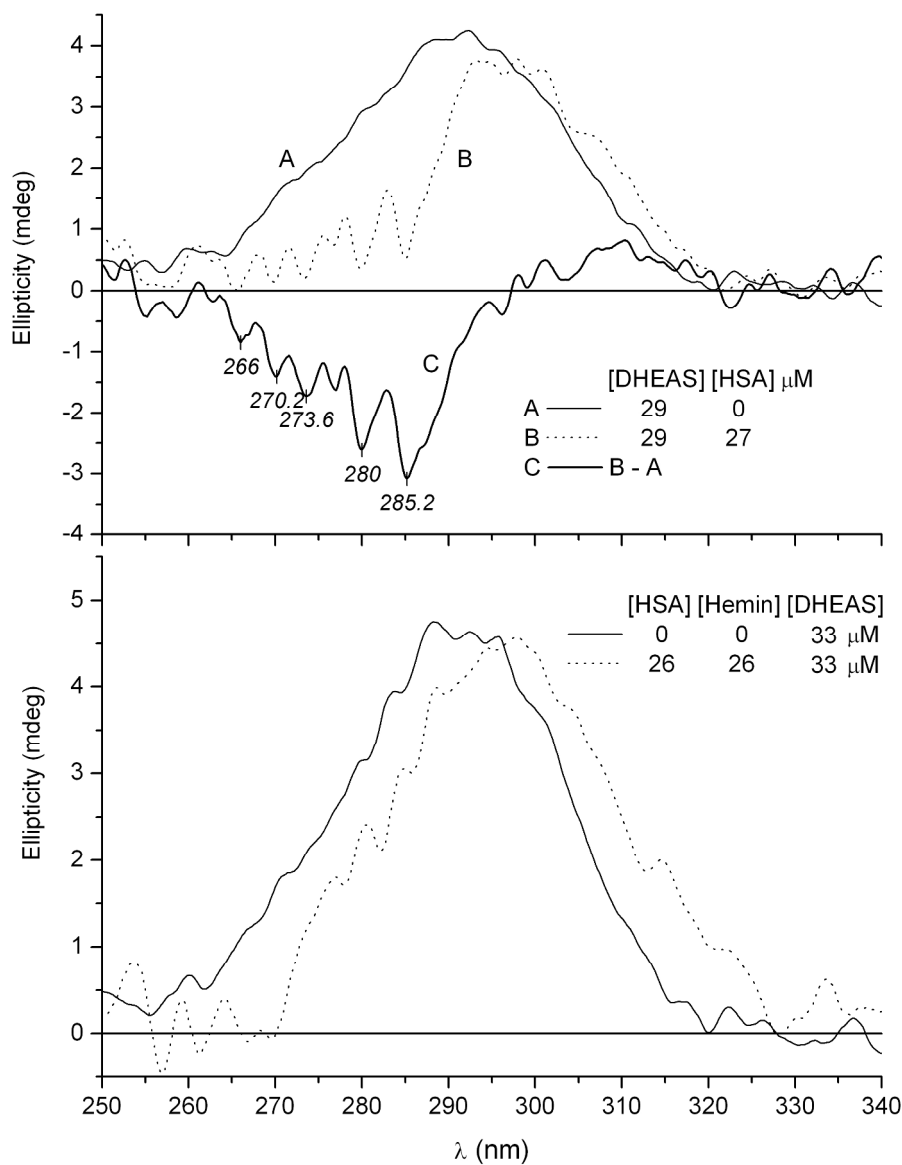


Figure 9
Top panel: CD band of DHEAS in the absence ('A') and in the presence ('B') of HSA (Ringer buffer, 25 °C).
Bottom panel: CD band of DHEAS in Ringer buffer and in hemin-HSA mixture (induced CD contribution of HSA bound hemin was subtracted).
990x1250mm (72 x 72 DPI)

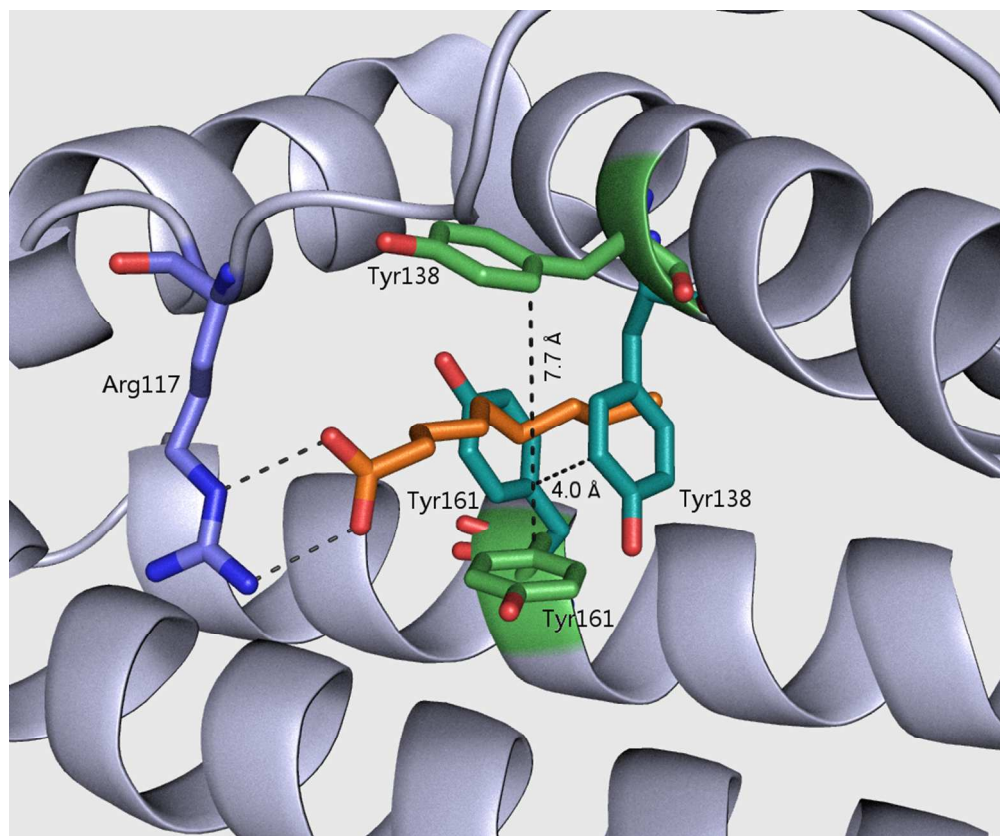
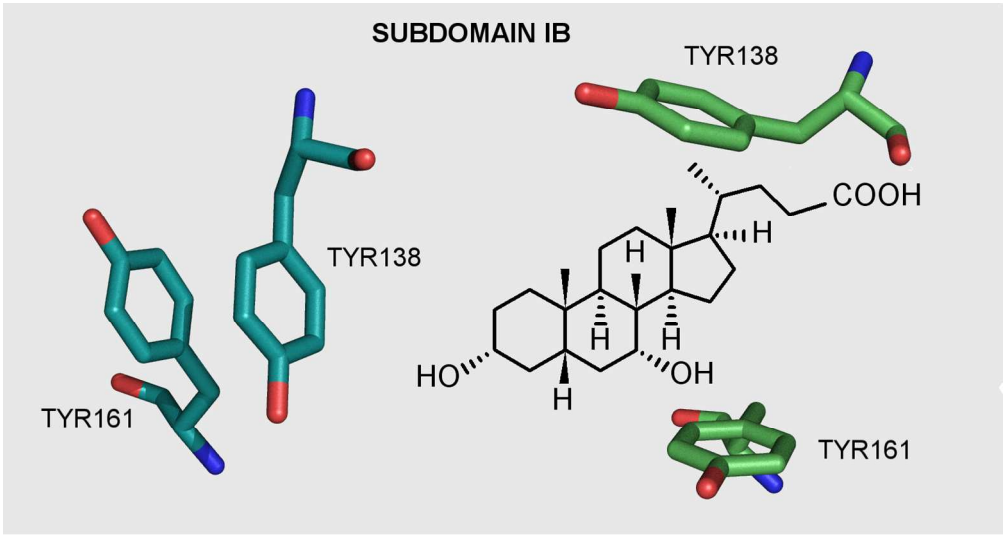


Figure 10

Superposition of subdomain IB of ligand-free HSA (PDB: 1E78, light blue tyrosines) and capric acid-HSA complex (PDB: 1E7E, green tyrosines) to illustrate the conformational re-arrangement of the Tyr138 and Tyr161 side chains. Note the large increase of the inter-residual distance upon insertion of the FA molecule (orange). H-bonds formed between capric acid and Arg117 are shown.



Graphic for the TOC entry
210x111mm (200 x 200 DPI)